



ELSEVIER

Available online at www.sciencedirect.com

ScienceDirect

journal homepage: <http://Elsevier.com/locate/radcr>

Case Report

Pyogenic brain abscess with atypical features resembling glioblastoma in advanced MRI imaging

Arsany Hakim MD^{a,*}, Markus Oertel MD^b, Roland Wiest MD^a

^a University institute for Diagnostic and Interventional Neuroradiology, Inselspital, Bern University Hospital, University of Bern, Freiburgstr. 10, CH-3010 Bern, Switzerland

^b Department of Neurosurgery, Inselspital, Bern University Hospital, University of Bern, Bern, Switzerland

ARTICLE INFO

Article history:

Received 27 September 2016

Received in revised form

28 November 2016

Accepted 19 December 2016

Available online 30 January 2017

Keywords:

Diffusion

Infectious

Neoplastic

Perfusion

Susceptibility

ABSTRACT

Differentiation between infectious and neoplastic brain processes is crucial for treatment planning. Advanced magnetic resonance imaging techniques, such as diffusion, perfusion, susceptibility weighted imaging, and magnetic resonance spectroscopy, enhance the imaging differences between these two pathologies. However, despite the utilization of these advanced techniques, the pathologic process may be confounded by atypical findings. Here, we report a case of an autistic patient with multiple brain lesions with diffusion weighted imaging, susceptibility weighted imaging, and perfusion patterns resembling features of a multicentric glioblastoma, which were confirmed surgically, neuropathologically, and bacteriologically as brain abscesses. We discuss the differentiation of these different entities in the light of advanced magnetic resonance imaging techniques.

© 2016 the Authors. Published by Elsevier Inc. under copyright license from the University of Washington. This is an open access article under the CC BY-NC-ND license (<http://creativecommons.org/licenses/by-nc-nd/4.0/>).

Case report

A 31-year-old autistic male patient presented with acute headache and fever. A contrast-enhanced computed tomography scan was performed and showed space-occupying lesions in the right parietal and left frontal lobes with ring enhancement and perifocal edema. The initial differential diagnosis was abscess versus multicentric glioblastoma. Laboratory analysis showed elevated C reactive protein levels (47 mg/L; normal range <5 mg/L) and a leukocyte count within the normal range. Preoperative clinical diagnosis was hindered and delayed most likely due to the patient's autism and impaired communication skills.

The patient subsequently underwent magnetic resonance imaging (MRI) (Avanto 1.5T, Siemens, Erlangen, Germany) to further differentiate these masses, which showed a multilocular lesion with a diameter of 4.5 cm in the left frontal lobe with marginal circular diffusion restriction and a reduced apparent diffusion coefficient (ADC) map and central increased diffusivity. The susceptibility weighted imaging (SWI) showed a peripheral irregular ring with a decreased signal and no dual rim sign. The perfusion parameters indicated a marked peripheral increased in relative cerebral blood volume (rCBV), with markedly increased leakage coefficient (K₂) in the ring lesion as well as in the surrounding extensive perifocal edema (Fig. 1). The ring enhancement was

Competing Interests: The authors have declared that no competing interests exist.

* Corresponding author.

E-mail address: arsany_hakim@yahoo.com (A. Hakim).

<http://dx.doi.org/10.1016/j.radcr.2016.12.007>

1930-0433/© 2016 the Authors. Published by Elsevier Inc. under copyright license from the University of Washington. This is an open access article under the CC BY-NC-ND license (<http://creativecommons.org/licenses/by-nc-nd/4.0/>).

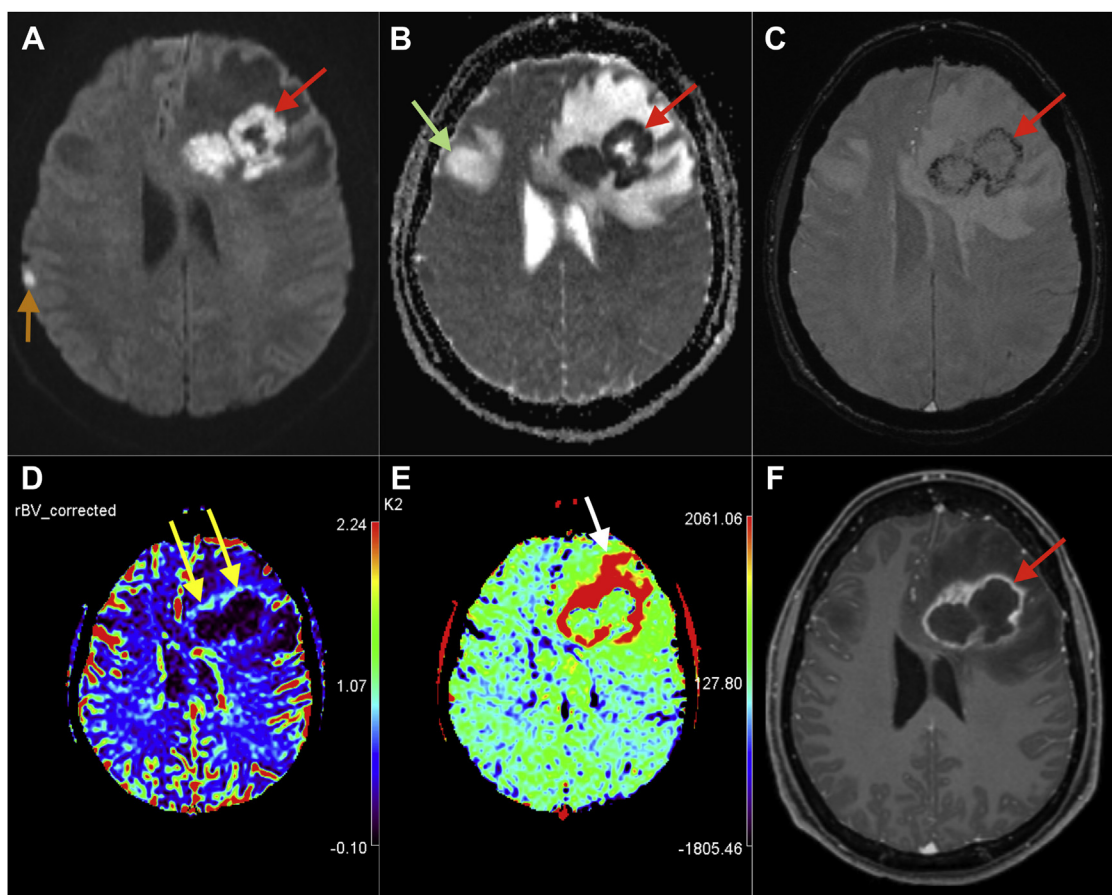


Fig. 1 – MRI with DWI (A), ADC (B), SWI (C), corrected rCBV (D), K2 (E) maps of dynamic susceptibility contrast-enhanced perfusion (DSC) obtained by OSVD deconvolution approach, and postcontrast T1 (F) showing atypical features of brain abscess (red arrows) with ring enhancement (F) and ring diffusion restriction with central increased diffusivity (A and B) as well as irregular hypointense circular ring in SWI (C). The rCBV is increased [yellow arrows in (D)] in the ventral part of the ring, and K2 is increased, extending to the neighboring edema [white arrow in (E)]. Notice the perifocal edema located cranially to another lesion in the right frontal lobe [green arrow in (B)] and a third smaller lesion with diffusion restriction in the right parietal lobe [orange arrow in (A)]. MRI, magnetic resonance imaging; DWI, diffusion weighted imaging; SWI, susceptibility weighted imaging; rCBV, relative cerebral blood volume; K2, leakage coefficient.

incomplete medially toward the lateral ventricle with increased signal intensity of the cerebrospinal fluid in the left frontal horn (Fig. 2). Other lesions with diffusion restriction were observed in the right frontal and parietal lobes with 2 cm and 6 mm diameters, respectively. Because of the emergency situation and the indication for immediate operation, additional MR spectroscopy was not performed.

Although the described imaging findings were atypical for an infectious process (no central diffusion restriction, no dual rim sign, and increased rCBV), the image features as a whole particularly the medially incomplete ring of enhancement and the clinical context clearly favored abscesses over multicentric glioblastoma or metastasis. For this reason, the patient underwent an emergency craniotomy with subsequent neuropathologic and microbiological examination, which confirmed the presence of intracranial abscesses with meningitis and ventriculitis. During the operation, evacuation of the frontal abscesses was performed, and a left-sided external ventricular drainage was placed. Bacteriological tests showed the presence of *Streptococcus milleri*. A follow-up MRI after the

craniotomy showed abscess evacuation but also signs of ischemia and increased intracranial tension due to prolonged preoperative raised intracranial pressure, perifocal edema, and herniation. Despite rapid, adequate, and intensive adjuvant therapy, the patient did not recover substantially and ultimately passed away 10 days thereafter.

Discussion

The differential diagnosis of multiple lesions with ring enhancement and prominent perifocal edema includes mainly infectious and neoplastic processes, such as brain abscess, metastasis, and multicentric glioblastoma [1,2]. Differentiation between these entities is of utmost importance to determine the indications and urgency of intervention and a suitable management plan. Advanced MRI techniques complement the role of conventional MRI in the differential diagnosis between these entities, and typically, more than one

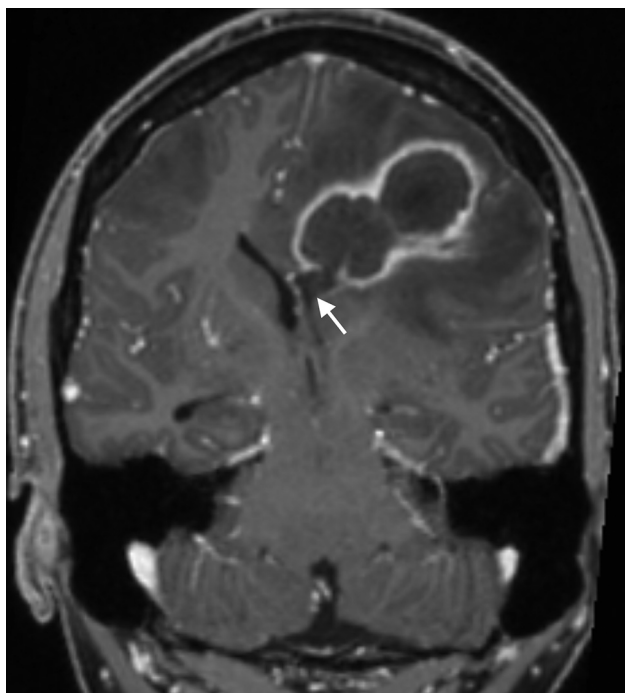


Fig. 2 – Coronal postcontrast T1 showing incomplete enhanced rim medially and increased CSF signal in the left ventral horn (arrow) consistent with ventriculitis. CSF, cerebrospinal fluid.

sequence is required to increase the sensitivity and specificity due to the complex pathogenesis of the disease process [3].

Diffusion weighted imaging (DWI) is based on the random Brownian motion of water molecules in a voxel of tissue; thus, it may provide information about the existing disease process according to the mobility of water within the lesion [4]. The usefulness of DWI in differentiating between brain abscesses and necrotic or cystic tumors has been previously proven with a sensitivity of 96% [5–7]. Depending on the stage of the abscess, the high cellularity and viscosity of the pus in the abscess cavity result in restricted diffusion, which appears hyperintense on the DWI and hypointense in ADC [4]. In contrast, necrotic tumor cysts demonstrate high diffusivity, that is, hypointense in DWI with an increased ADC value. A low diffusion signal similar to brain tumors has been reported in approximately 5%–21% of untreated abscesses [8]. Higher ADC values are found in fungal abscesses than in bacterial abscesses [9]. Lesions with ring pattern in DWI have a broad spectrum of differential diagnoses. In immunocompetent patients, the differential diagnosis includes mainly demyelinating diseases and stroke, but only in 3% of cases pyogenic abscesses [10].

SWI is designed by combining the gradient echo data of phase and magnitude [11]. It utilizes the susceptibility differences between tissues to obtain an intrinsic imaging contrast. SWI is sensitive to the differences between paramagnetic substances such as iron and blood products, which have positive susceptibility, that is, appear hypointense, and diamagnetic substances, such as calcium, water, and other tissue contents, which have negative susceptibility [11,12]. Because angiogenesis is a hallmark of aggressive tumors, such

as glioblastoma, SWI is helpful in detecting blood products associated with this pathologic process [12]. The random deposition of hemorrhagic products in glioblastoma causes the presence of a hypointense rim surrounding the necrotic center, which is usually irregular and incomplete, in contrast to the hypointense rim present in brain abscess, which is usually smooth and complete [13]. Pyogenic brain abscess, and not glioblastoma, has a characteristic appearance of a concentric hypointense rim surrounding a hyperintense rim. This appearance is called a “dual rim sign” and is found in the SWI due to its sensitivity to both paramagnetic and diamagnetic substances [13]. The end products by macrophages of paramagnetic free radicals have been proposed to be responsible for the hypointense rim, and the granulation tissues between the necrotic center and fibrocollagenous capsule are most likely responsible for the hyperintense signal [13,14]. The dual rim sign has been reported to be the most specific feature in differentiating brain abscess from glioblastoma on SWI [13].

Perfusion imaging enables the measurement of tissue microcirculation. The most widely used perfusion technique in MRI is the dynamic susceptibility contrast imaging [15]. It uses the signal intensity loss in T2* gradient recalled echo, which occurs dynamically after injecting a bolus of contrast. The role of perfusion imaging, specifically the calculated rCBV, is an estimation of the angiogenesis, which is a marker for aggressive tumors, in which the enhancing rim contains viable tumors, thereby demonstrating an increased rCBV. In contrast to the brain abscess and its enhancing rim, which lacks neo-vascularization and histologically the microvascular density is markedly lower than in glioblastoma, and thus, it demonstrates lower rCBV values on the enhancing rim compared to glioblastoma [8]. Underestimation of rCBV may occur due to a signal intensity increase secondary to the T1 effect, which occurs in pathologies with blood–brain barrier breakdown and contrast leakage. Thus, a higher accuracy can be achieved by calculating (K2). The increase in vascular permeability in both abscess and glioblastoma correlates with an increase in K2 in enhancing rims and adjacent edema, but metastasis shows an increase in K2 only in the enhancing rim [8]. In summary, the corrected rCBV demonstrates different values between neoplastic and infectious processes, but the K2 values are the same.

Table 1 summarizes the differences between pyogenic brain abscess and glioblastoma based on the discussed three advanced MRI sequences.

Table 1 – Summary of the typical features and differentiation between glioblastoma and abscess by advanced MRI techniques.

| | Glioblastoma | Abscess |
|--|--|---|
| DWI | Low signal | Restriction in central abscess cavity |
| SWI | Incomplete irregular hypointense rim No dual rim sign | Complete smooth hypointense rim Dual rim sign |
| PWI | Higher rCBV values increased K2 | Lower rCBV values than glioblastoma increased K2 |
| DWI, diffusion weighted imaging; SWI, susceptibility weighted imaging; PWI, perfusion weighted imaging; rCBV, relative cerebral blood volume; K2, leakage coefficient. | | |

Table 2 – Summary of the four stages of brain abscess with radiological and pathological correlation (modified from Osborn's brain [19]).

| | Early cerebritis | Late cerebritis | Early capsule | Late capsule |
|--------------------|--|--|--|---|
| Duration | 3–5 d | 4–14 d | 2 wk–2 mo | Weeks–months |
| Pathology | <ul style="list-style-type: none"> - Focal unencapsulated infection - Edematous hyperemic mass - Patchy necrotic foci - Petechial hemorrhage | <ul style="list-style-type: none"> - Necrotic foci coalescence forming necrotic core - Core surrounded by a poorly organized rim of inflammatory cells, macrophages, granulation tissues, and fibroblasts - Capillary proliferation and surrounding vasogenic edema | <ul style="list-style-type: none"> - Necrotic core liquefaction - Granulation tissue proliferation around the rim - Presence of a well-delineated collagenous capsule | <ul style="list-style-type: none"> - Gradual involution and shrinkage of the central cavity with treatment - Collagen deposition further thickens the wall - Persistence of small gliotic nodule of collagen and fibroblasts |
| Imaging morphology | Poorly margined mass | <ul style="list-style-type: none"> - Better delineated mass - Surrounding edema | <ul style="list-style-type: none"> - Well-delineated round or ovoid mass with core - Smooth, complete thin rim, that is thinnest on its ventricular side | <ul style="list-style-type: none"> - Cavity collapses - Capsule thickens - Overall mass diminishes in size and gradually disappears |
| T1 | Hypointense/isointense | <ul style="list-style-type: none"> - Center: hypointense - Rim: isointense/mildly hyperintense | <ul style="list-style-type: none"> - Center: hyperintense - Rim: isointense/hyperintense | |
| T2 | Hyperintense | <ul style="list-style-type: none"> - Center: hyperintense - Rim: hypointense | <ul style="list-style-type: none"> - Center: hyperintense - Rim: hypointense | |
| GRE/SWI | Hemorrhagic foci | | Dual rim sign | |
| DWI | Restriction | Restriction | Center: strong restriction | |
| Contrast | Patchy enhancement | <ul style="list-style-type: none"> - Intense irregular ring enhancement - Delayed imaging: progression of contrast from periphery to center | Thin enhancing rim | Possible persistence of resolving abscess for months after clinical symptoms have resolved |
| Advanced imaging | <ul style="list-style-type: none"> - PWI: wall: lower rCBV than enhancing tumor - MRS: necrotic core: amino acid, lactate, acetate, and succinate - FA: increased in abscess cavity | | | |

GRE, gradient recalled echo; PWI, perfusion weighted imaging; DWI, diffusion weighted imaging; SWI, susceptibility weighted imaging; MRS, magnetic resonance spectroscopy; FA, fractional anisotropy.

Ozbayrak et al. [16] reported a case of atypical presentation of brain abscess in DWI and PWI, but with a dual rim sign. Our patient showed atypical presentations in all three sequences. In DWI, it was atypical due to the presence of ring diffusion restriction and increased central diffusivity, while in SWI, it was atypical due to the absence of the dual rim sign and the presence of an irregular hypointense ring. In the PWI, it was atypical due to the higher rCBV value than expected for an abscess.

Originally described in animal models and later in humans, the development of pyogenic brain abscess passes through four stages: early cerebritis, late cerebritis, early capsule, and late capsule [17,18]. Imaging features evolve over time, and the appearance during MRI varies widely between these four stages (Table 2) [19]. This variation may affect the specificity of imaging signs described in the literature. In the early capsule stage, the abscess rim enhances strongly and is thinnest on its ventricular side, which may rupture causing ventriculitis, as in the presented case [2]. A possible cause of the atypical feature in DWI in our case is that the abscess ruptured causing the abscess contents to flow into the ventricle, which may have also caused admixing of pus with cerebrospinal fluid inside the abscess cavity, thus causing increased diffusivity in the center of the abscess.

The imaging findings on the SWI are dependent on magnetic strength [14] with more sensitive results on 3T [20]. The study showing the dual rim sign by Toh et al. was performed on 3T, and our examination was performed on 1.5T. Bleeding on the abscess wall may also cause atypical findings [21]. Another possible cause for the irregularity on the SWI could be the reduced pressure inside the abscess cavity after rupture into the ventricle, causing irregularity of the abscess membrane and therefore disorganization of the deposited paramagnetic free radicals.

Perfusion measurement is a complex process in which many factors may lead to abnormal findings, including the specific technique used [22]. Cianfoni et al. [23] reported a case of nocardial brain abscess with increased vascularity in the enhancing rim of the lesion showing increased rCBV. Muccio et al. [24] reported brain abscess in the early capsular stage with increased rCBV resembling a necrotic tumor. In both cases, the enhancing rim was thin. The presumed explanation was that the abscess was in the early capsular stage [24]. In the presented case, the area with increased rCBV is corresponded to the thickest part of the enhancing rim (Figs. 1D and F), which may represent a relative increase in capillary density, thus increasing the rCBV.

Teaching point

Although advanced MRI techniques provide valuable information for differentiating pyogenic brain abscess from neoplastic lesions, atypical findings must be taken into account. Thus, correlation with conventional MRI sequences and consideration of the clinical picture are of utmost importance in determining the adequate management strategy.

REFERENCES

- [1] Schwartz KM, Erickson BJ, Lucchinetti C. Pattern of T2 hypointensity associated with ring-enhancing brain lesions can help to differentiate pathology. *Neuroradiology* 2006;48:143–9.
- [2] Smirniotopoulos JG, Murphy FM, Rushing EJ, Rees JH, Schroeder JW. Patterns of contrast enhancement in the brain and meninges. *Radiographics* 2007;27:525–51.
- [3] Huisman TAGM. Tumor-like lesions of the brain. *Cancer Imaging* 2009;9:S10–3.
- [4] Schaefer PW, Grant PE, Gonzalez RG. Diffusion-weighted MR imaging of the brain. *Radiology* 2000;217:331–45.
- [5] Ebisu T, Tanaka C, Umeda M, Kitamura M, Naruse S, Higuchi T, et al. Discrimination of brain abscess from necrotic or cystic tumors by diffusion-weighted echo planar imaging. *Magn Reson Imaging* 1996;14:1113–6.
- [6] Chang SC, Lai PH, Chen WL, Weng HH, Ho JT, Wang JS, et al. Diffusion-weighted MRI features of brain abscess and cystic or necrotic brain tumors: comparison with conventional MRI. *Clin Imaging* 2002;26:227–36.
- [7] Reddy JS, Mishra AM, Behari S, Husain M, Gupta V, Rastogi M, et al. The role of diffusion-weighted imaging in the differential diagnosis of intracranial cystic mass lesions: a report of 147 lesions. *Surg Neurol* 2006;66:246–50.
- [8] Toh CH, Wei K-C, Chang C-N, Ng S-H, Wong H-F, Lin C-P. Differentiation of brain abscesses from glioblastomas and metastatic brain tumors: comparisons of diagnostic performance of dynamic susceptibility contrast-enhanced perfusion MR imaging before and after mathematic contrast leakage correction. *PLoS One* 2014;9:e109172.
- [9] Mueller-Mang C, Castillo M, Mang TG, Cartes-Zumelzu F, Weber M, Thurnher MM. Fungal versus bacterial brain abscesses: is diffusion-weighted MR imaging a useful tool in the differential diagnosis? *Neuroradiology* 2007;49:651–7.
- [10] Finelli PF, Foxman EB. The etiology of ring lesions on diffusion-weighted imaging. *Neuroradiol J* 2014;27:280–7.
- [11] Liu C, Li W, Tong KA, Yeom KW, Kuzminski S. Susceptibility-weighted imaging and quantitative susceptibility mapping in the brain. *J Magn Reson Imaging* 2015;42:23–41.
- [12] Mohammed W, Xunning H, Haibin S, Jingzhi M. Clinical applications of susceptibility-weighted imaging in detecting and grading intracranial gliomas: a review. *Cancer Imaging* 2013;13:186–95.
- [13] Toh CH, Wei KC, Chang CN, Hsu PW, Wong HF, Ng SH, et al. Differentiation of pyogenic brain abscesses from necrotic glioblastomas with use of susceptibility-weighted imaging. *Am J Neuroradiol* 2012;33:1534–8.
- [14] Robinson RJ, Bhuta S. Susceptibility-weighted imaging of the brain: current utility and potential applications. *J Neuroimaging* 2011;21:e189–204.
- [15] Svolos P, Kousi E, Kapsalaki E, Theodorou K, Fezoulidis I, Kappas C, et al. The role of diffusion and perfusion weighted imaging in the differential diagnosis of cerebral tumors: a review and future perspectives. *Cancer Imaging* 2014;14:20.
- [16] Ozbayrak M, Ulus OS, Berkman MZ, Kocagoz S, Karaarslan E. Atypical pyogenic brain abscess evaluation by diffusion-weighted imaging: diagnosis with multimodality MR imaging. *Jpn J Radiol* 2015;33:668–71.
- [17] Britt RH, Enzmann DR, Yeager AS. Neuropathological and computerized tomographic findings in experimental brain abscess. *J Neurosurg* 1981;55:590–603.
- [18] Britt RH, Enzmann DR. Clinical stages of human brain abscesses on serial CT scans after contrast infusion. Computerized tomographic, neuropathological, and clinical correlations. *J Neurosurg* 1983;59:972–89.

-
- [19] Osborn AG. Congenital, acquired pyogenic and acquired viral infections. In: Osborn A, editor. *Osborn's brain Imaging, Pathol. Anat.* Salt Lake City: Amirsys; 2012. p. 313–7.
- [20] Deistung A, Rauscher A, Sedlacik J, Stadler J, Witoszynskij S, Reichenbach JR. Susceptibility weighted imaging at ultra high magnetic field strengths: theoretical considerations and experimental results. *Magn Reson Med* 2008;60:1155–68.
- [21] Thamburaj K, Agarwal AK, Sabat SB, Nguyen DT, Thamburaj K, Agarwal AK, et al. Hemorrhage in the wall of pyogenic brain abscess on susceptibility weighted MR sequence: a report of 3 cases. *Case Rep Radiol* 2014;2014:907584.
- [22] Essig M, Shiroishi MS, Nguyen TB, Saake M, Provenzale JM, Enterline D, et al. Perfusion MRI: the five most frequently asked technical questions. *Am J Roentgenol* 2013;200:24–34.
- [23] Cianfoni A, Calandrelli R, De Bonis P, Pompucci A, Lauriola L, Colosimo C, et al. Nocardia brain abscess mimicking high-grade necrotic tumor on perfusion MRI. *J Clin Neurosci* 2010;17:1080–2.
- [24] Muccio CF, Leonini S, Esposito G, Cerase A. Pyogenic abscess from *Providencia stuartii* mimicking necrotic tumour at perfusion-weighted imaging. *Neurol Sci* 2011;32:919–23.